Journal of the European Ceramic Society 20 (2000) 1327–1331

Phase formation and microstructural evolution of R-α'-AlN-polytypoid ceramics (R = Y, Y + Sm and Sm)

Wei-wu Chen, Ya-wen Li, Wei-ying Sun *, Dong-sheng Yan

The State Key Laboratory of High Performance Ceramics and Superfine Microstructure, Shanghai Institute of Ceramics, Shanghai 200050, PR China

Received 5 August 1999; received in revised form 10 November 1999; accepted 29 December 1999

Abstract

In the present work, Y, Sm and (Y + Sm) were separately used to explore the effects of rare-earth elements on the reaction sequence and microstructural evolution in α-sialon-AlN-polytypoid composite ceramics. The results showed that the reaction sequences in the composite ceramics are affected by rare earth elements. With the existence of AlN-polytypoid α-sialon develops into elongated morphology. The Sm–α-sialon composition exhibits the feature of fine grains with high aspect ratio and Y-composition possesses rather coarse morphology with low aspect ratio. In the composite ceramics, AlN-polytypoid was not distributed homogeneously around the α-sialon grains, especially in the Y-composition. The variation in microstructure with rare-earth elements in the Sialon materials was discussed based on their reaction sequences.

Keywords: AlN polytypoid; Microstructure-final; Rare earths; Sialon

1. Introduction

α-Sialon (α'), as one of the most attractive high-temperature structure materials,[1] has some unique characteristic, such as high hardness and the potential of cleaning up grain boundary. However, the flexure strength and toughness of α-sialon are relatively low, which is thought to be related to its microstructure of equi-axed shape grains. It is well recognized that the elongated grains in microstructures might in situ toughen materials through the effect of some mechanisms such as crack bridging, crack deflection and grain pullout.[2] α-Sialon materials should be toughened by in-situ growth of elongated grains as well. AlN-polytypoids, despite the relatively low mechanical properties, afford the potential of toughening α-sialon ceramics because they possess fiber-like morphology. Our previous work[3] indicated that with less than 10 wt% addition of 12H ($SiAl_5O_2N_2$) into α-sialon composition, the resulting composite ceramics showed obvious enhancement in toughness and slight decrease in hardness. Furthermore, in our resent work, some interesting characteristics of AlN-polytypoids were observed. Their high temperature strength is higher than room temperature strength; moreover, they can promote the formation of elongated α-sialon when they are incorporated into α-sialon.[4,5] However, the microstructure of the α'-12H materials is non-uniform, which inevitably has a negative effect on the mechanical property.[6] In fabrication of Sialon ceramics, the ternary eutectic melt of M_2O_3–Al_2O_3–SiO_2, which may preferentially wet either Si_3N_4 or AlN, play an important role in determining the reaction pathway.[7] The alkalinity of M element in the melt was found to control the wetting behavior. Based on the surface oxides on nitrides, Si_3N_4 has stronger acidity than AlN and the alkalinity of rare earth elements decreases with increasing atomic number. Therefore, the phase formation and microstructural evolution in the α-AlN-polytypoid composite ceramics might be affected by rare earth elements. Motivated by the above studies, Y (with similar behavior to heavy rare earth element), Sm (a typical light rare earth element) and Y + Sm(dual-rare earth elements) were selected to prepare the α'-AlN-polytypoid composite ceramics with the aim of understanding the effect of rare earth elements on densification, phase formation and microstructural evolution of Sialon ceramics.

---

* Corresponding author. Tel.: +86-21-62512990 ext. 6224; fax: +86-21-6281-3903.

E-mail address: wysun@sunm.shcnc.ac.cn (W. Sun).

PII: S0955-2219(00)00006-6

2. Experimental

The phase relationships[8,9] indicated that the oxygen-rich α-sialon is compatible with AlN-polytypoids, which start from 12H in the Y–Si–Al–O–N system and from 21R in Sm–Si–Al–O–N. The YAG and $SmAlO_3$ were used as sintering additives for Y- and Sm- compositions respectively. For comparison, the same nominal composition of 90 wt% α-sialon ($m=1$, $n=1.7$)-10 wt% 12H with extra 2.5 wt% additives was used for the different systems, as listed in Table 1. The starting powders were α-Si_3N_4 (UBE-10, $\alpha>95$ wt%, 2.0 wt% O), Al_2O_3 (99.99%), AlN(1.3 wt% O) and Ln_2O_3 (99.99%) where Ln = Y and Sm. The oxygen contents of the nitride powders were taken into account in computing the compositions. Powder mixtures were milled with absolute alcohol in an agate mortar for 1.5 h and dried under an infrared lamp. Compacted pellets of dried powders were hot-pressed (HP) in the range of 1450–1800°C at an interval of 100°C for 1 h under a pressure of 20 MPa in a graphite resistance furnace. After sintering, the specimens were cooled down in the furnace at a rate of ~50°C/min.

Bulk densities of the samples were measured according to the Archimedes principle. Phase identification was performed by X-ray diffraction (XRD) using an RAX-10 diffractometer. Semi-quantitative analysis of crystalline phase content was based on the calibration curves. The polished surfaces of the fired specimens were either etched by molten NaOH or directly used for microstructural observation under the scanning electron microscope (SEM; KYKY200) equipped with energy-dispersive spectrometers (EDS; Link OXFORD).

3. Results and discussion

3.1. Reaction sequence and densification

The densification curves and reaction sequences for these three compositions are shown in Figs. 1 and 2 respectively. As shown, the Y + Sm-composition reached full density at 1550°C, which is 100°C lower than in the Y- and Sm-composition. As expected, dual-elements

Table 1
Designed phase compositions of samples

Specimens	Phase design wt%		Sintering additive wt%	
	α' ($m=1$, $n=1.7$)	12H	YAG	$SmAlO_3$
Y-composition	90	10	2.5	
Y + Sm-composition[a]	90	10	1.25	1.25
Sm-composition	90	10		2.5

[a] Y:Sm = 1:1, in mol.

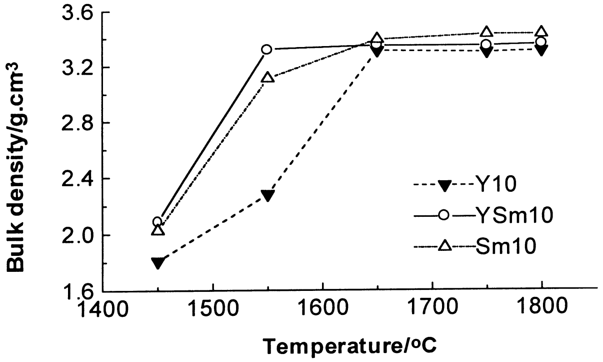

Fig. 1. Densification behavior of the different compositions.

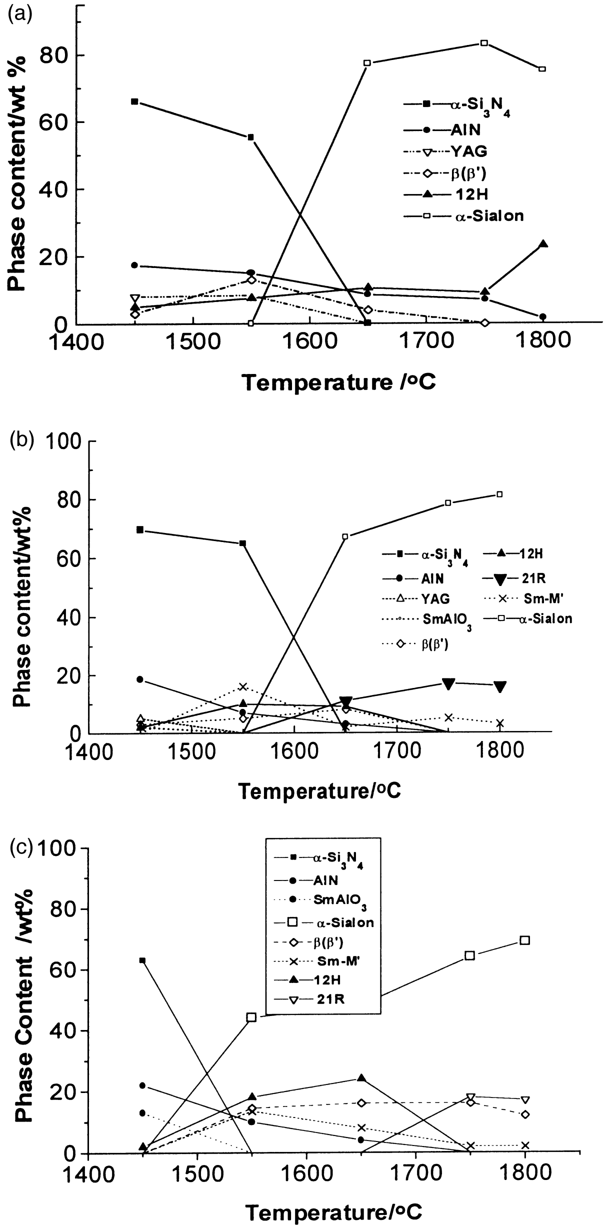

Fig. 2. Reaction sequence of: (a) Y-composition; (b) Y + Sm-composition; (c) Sm-composition.

can reduce the eutectic point of the oxides, thus promoting the dissolution of α-Si_3N_4 and AlN. As indicated, in the Sm-composition, the dissolution of α-Si_3N_4 was quite rapid and α-sialon forms simultaneously with 12H, while in the Y-composition, the dissolution of α-Si_3N_4 was relatively more sluggish, and the formation of α-sialon was consequently behind 12H. The formation priority of 12H degraded in the Y + Sm-composition than in Y-composition. The variation in the α-Si_3N_4 dissolution rate in the three compositions is in agreement with the acid–alkali principle. Sm has stronger alkalinity than Y and thus makes α-Si_3N_4 dissolve more easily. However, the formation rate of α-sialon is not merely dependent on the dissolution rate of α-Si_3N_4 but affected by the different ability in the formation of Ln-α-sialon as well, especially in the Sm-composition. As is known, the difference of ionic radius of Y (0.93 Å) and Sm (1.04 Å) in this study results in their different capability to form α-sialon. Y^{3+} can enters α-sialon more easily and Y-α-sialon is stable even at a relative low temperature. Sm^{3+} enters α-sialon with difficulty because of its big ionic radius and Sm-α-sialon is only stable at high temperature in response to its larger lattice vacancy along with the strenuous atomic vibration. Moreover, the formation of Sm-M′(melilite, $Sm_2Si_{3-x}Al_xO_{3+x}N_{4-x}$, $x < 0.9$) and β′ is a strong competitor with α-sialon for Si_3N_4 in Sm-composition. This is in agreement with other previous works.[10] Consequently, in the Y- and (Y + Sm)-compositions, at the temperature range 1550–1650°C α-sialon formed rapidly with the dissolution of Si_3N_4, and the content of α-sialon reached 78wt% and 67 wt% respectively, much higher than the Sm-α-sialon content (48 wt%) at the same temperature range. At high temperatures, with the dissolution of intermediate phases and AlN, the final phase assemblages reached equilibrium. The lower content of α-sialon obtained in the samples than the designed value

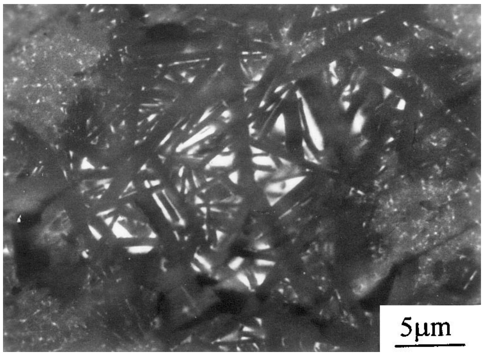

Fig. 4. Back-scattered SEM micrographs showing the agglomerated AlN-polytypoid dark: AlN-polytypoids; grey: α-sialon; white: glass.

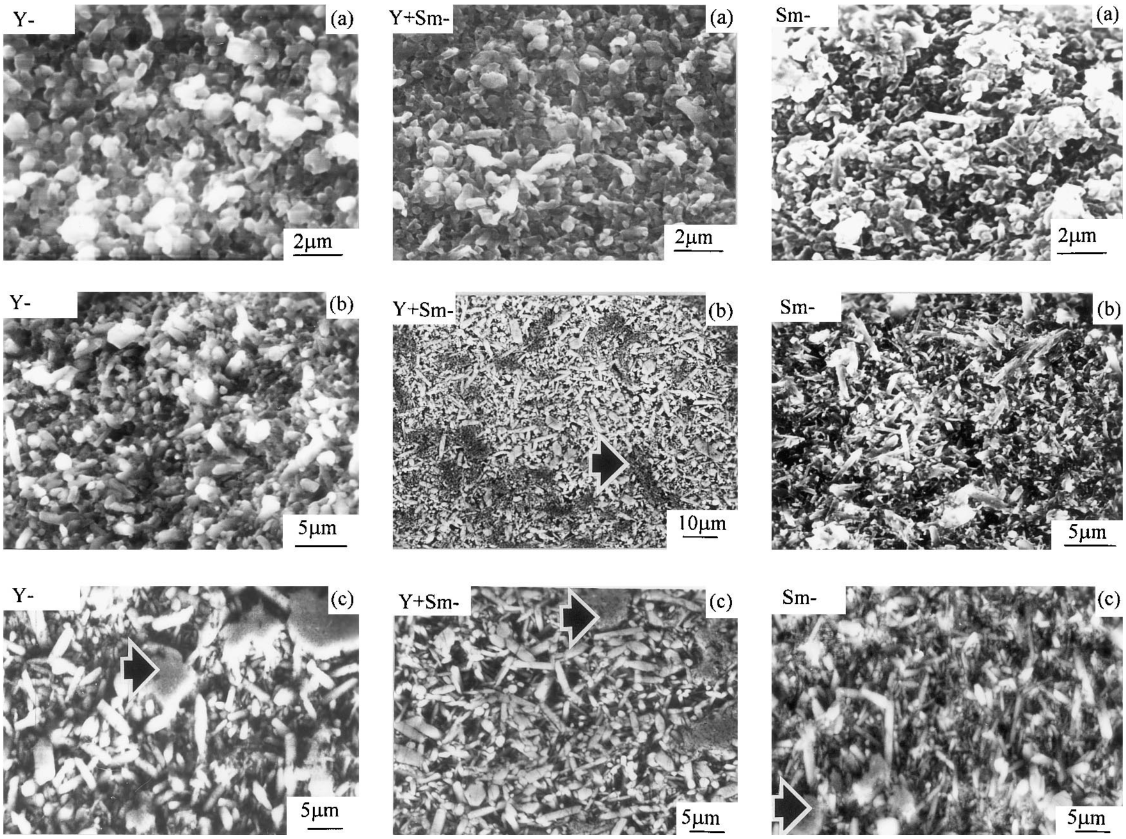

Fig. 3. Microstructural evolution of Ln-α-Sialon-AlN-polytypoid hot pressed at (a) 1650°C; (b) 1750°C; (c) 1800°C dark agglomerated particles: AlN-polytypoid (denoted with an arrow); white grains: α-sialon.

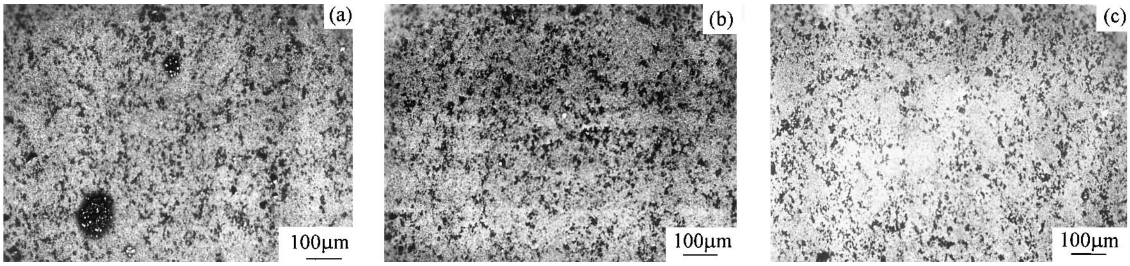

Fig. 5. Microstructure of Ln-α-sialon-AlN-polytypoid hot-pressed at 1800°C, showing the distribution of AlN-polytypoid in: (a) Y-composition; (b) Y + Sm-composition; (c) Sm-composition.

can be attributed to the formation of Ln-sialon liquid phase.

3.2. Microstructural evolution

The typical microstructural evolution of the three compositions is shown in Fig. 3. As indicated, the influence of different rare earth elements on morphology of α-sialon grains can be found. At 1650°C, α-sialon grains were small and the grain diameter was about 600 450 and 300 nm in the Y-, (Y + Sm)- and Sm-composition respectively. Moreover, the Sm-α-sialon already showed the trend to form an elongated morphology. At 1750°C, α-sialon grains grew and the elongated morphology was also observed in the (Y + Sm)-composition. At 1800°C, the elongated α-sialon grains occurred in the Y-composition as well. Despite the formation of elongated α-sialon in all compositions there exist some differences in the size and aspect ratio of elongated grains. The Sm-composition exhibited the feature of fine grains with a high aspect ratio and the Y-composition possessed a rather coarse morphology with a low aspect ratio. This can be attributed to the reaction competition of 12H with α-sialon and the different ability in the formation of Ln-α-sialon, as mentioned above. In the Sm-composition, more α-sialon nuclei at lower temperature made Sm-α-sialon develop into fine grains at high temperature. Meanwhile, the difficulty of Sm entering into α-sialon led to a relatively low driving force for the growth of Sm-α-sialon and this possibly results in elongated Sm-α-sialon grains with a high aspect ratio. In the Y-composition, α-sialon started to form at a rather high temperature, and with increasing temperature, it rapidly precipitated and grew. This might result in its coarse grain microstructure. This is in agreement with the results obtained by Zhang,[11] who observed that Sm-α-sialon grains were finer than Dy-α-sialon grains. The dark agglomerated particles (denoted with arrows in Fig. 3), which were broken by the etching of NaOH, were identified as AlN-polytypoid by EDS. The back-scattered SEM micrographs of the un-etched sample surface are shown in Figs. 4 and 5. As indicated, the distribution of AlN-polytypoid was not homogeneous and the extent of the non-uniform distribution decreased in the sequence of Y-, (Y + Sm)- and Sm-composition. The preferential formation of AlN-polytypoid in the composite ceramics might be the main cause for its non-uniform distribution.

4. Conclusion

The effect of different rare earth elements on phase formation and microstructural evolution in three Ln-α-sialon–AlN-polytypoid compositions is obvious. In the Sm-composition, α-Si_3N_4 dissolved quickly and disappeared at 1550°C; α-sialon and 12H occurred simultaneously. In the Y-composition, α-Si_3N_4 completely disappeared at 1650°C; 12H formed earlier than α-sialon. The formation priority of 12H degraded in the Y + Sm-composition. α-Sialon developed into an elongated morphology at high temperatures in all compositions. The Sm-composition exhibited the feature of fine grains with a high aspect ratio and the Y-composition possessed rather coarse morphology with a low aspect ratio. With the addition of Sm into the Y-composition, its microstructure also slightly changed towards that of the Sm-composition. In the composite ceramics, the AlN-polytypoid phase was not distributed homogeneously around the α-sialon grains, especially in the Y-composition. In the Sm-composition, this non-uniform microstructure improved.

Acknowledgements

Financial support for the research was obtained from the National Natural Science Foundation of China. The authors would also like to thank Dr. Yi-Bing Cheng of Monash University for fruitful discussion.

References

1. Cao, G. Z. and Metselaar, R., α′-Sialon ceramics: a review. *Chem. Mater.*, 1991, **3**, 242–252.
2. Becher, P. F., Design of toughened ceramics. *J. Am. Ceram. Soc.*, 1991, **74**, 255–269.
3. Li, H. X., Sun, W. Y., Yan, D. S. and Tien, T. Y., Fabrication and mechanical properties of α′-sialon-12H multiphase ceramics.

In *Proceedings of the 5th International Symposium on Ceramic Materials and Components for Engines*, ed. D. S. Yan. World Scientific, Shanghai, 1995, pp. 194–197.

4. Li, H. X., Sun, W. Y. and Yan, D. S., Mechanical properties of hot-pressed 12H ceramics. *J. Eur. Ceram. Soc.*, 1998, **15**, 697–701.
5. Chen, W. W., Sun, W. Y. and Yan, D. S., Submitted to *Mater. Letters*.
6. Li, H. X., Study and design of toughened–sialon-AlN-polytypoid dual-phase ceramics. PhD thesis, Shanghai Institute of Ceramics, Shanghai, 1994.
7. Menon, Mohan and Chen, I-Wei, Reaction densification of α-sialon: I, wetting behavior and acid-base reactions. *J. Am. Ceram. Soc.*, 1995, **78**, 545–552.
8. Sun, W. Y., Tien, T. Y. and Yan, D. S., Subsolidus phase relationships in part of the system Si,Al,Y/N,O: the system Si3N4-AlN-YN-Al2O3-Y2O3. *J. Am. Ceram. Soc.*, 1991, **11**, 2753–2758.
9. Cheng, Y. B. and Thompson, D. P., Preparation and grain boundary heat treatment of samarium α-sialon ceramics. *J. Eur. Ceram. Soc.*, 1994, **14**, 13–21.
10. Wang, P. L., Sun, W. Y. and Ten, T. S., Sintering and formation of R-α′-Sialons (R = Nd, Sm, Gd, Dy, Er and Yb). *Eur. J. Solid State Inorg. Chem.*, 1994, **31**, 93–104.
11. Zhang, C., Sun, W. Y. and Yan, D. S., Optimizing mechanical properties and thermal stability of Ln-α-β-sialon by using duplex Ln elements (Dy and Sm). *J. Eur. Ceram. Soc.*, 1999, **19**, 33–39.